International Journal of Naval Architecture and Ocean Engineering 13 (2021) 50–56

Contents lists available at ScienceDirect

International Journal of Naval Architecture and Ocean Engineering

journal homepage: http://www.journals.elsevier.com/international-journal-of-naval-architecture-and-ocean-engineering/

Accuracy evaluation of 3D time-domain Green function in infinite depth

Teng Zhang [a], Bo Zhou [a, *], Zhiqing Li [a], Xiaoshuang Han [b], Wie Min Gho [c]

[a] State Key Laboratory of Structural Analysis for Industrial Equipment, School of Naval Architecture Engineering, Dalian University of Technology, Dalian, 116024, China
[b] Marine Engineering College, Dalian Maritime University, Dalian, 116026, PR China
[c] Maritime Production research Pte. Ltd, 915806, Singapore

ARTICLE INFO

Article history:
Received 17 August 2020
Received in revised form
8 November 2020
Accepted 30 November 2020
Available online 2 February 2021

Keywords:
Time-domain Green function
Asymptotic expansion
Taylor series expansion
Ordinary differential equation
Radiation problem

ABSTRACT

An accurate evaluation of three-dimensional (3D) Time-Domain Green Function (TDGF) in infinite water depth is essential for ship's hydrodynamic analysis. Various numerical algorithms based on the TDGF properties are considered, including the ascending series expansion at small time parameter, the asymptotic expansion at large time parameter and the Taylor series expansion combines with ordinary differential equation for the time domain analysis. An efficient method (referred as "Present Method") for a better accuracy evaluation of TDGF has been proposed. The numerical results generated from precise integration method and analytical solution of Shan et al. (2019) revealed that the "Present method" provides a better solution in the computational domain. The comparison of the heave hydrodynamic coefficients in solving the radiation problem of a hemisphere at zero speed between the "Present method" and the analytical solutions proposed by Hulme (1982) showed that the difference of result is small, less than 3%.

1. Introduction

An efficient hydrodynamic analysis is essential to determine the interaction of flow and ship structure for the safe design of ship operation in water (Zhang et al., 2019). As the 3D TDGF is simpler and requires less computational efforts than the frequency domain Green function approach, it has been widely used in the hydrodynamic analysis of ships with the effect of constant forward speed in the time-domain environment. Some of the research works related to this subject in the past included the time domain analysis of ship motions by Liapis (1986) and Datta et al. (2011), the time domain analysis of wave exciting forces on ships by King (1987), a comparative linear and nonlinear ship motions by Singh and Sen, (2007) and the study of ship motions with forward speed by Sun and Ren (2018). As the use of time-domain panel method requires much computational efforts for solving the boundary element integral equation in thousands of time steps, an accuracy evaluation of 3D TDGF is necessary for the efficient hydrodynamic analysis of ships.

For solving the linear time-domain problem in hydrodynamic analysis, the linearization of boundary conditions of 3D TDGF would first have to be obtained (Wehausen and Laitone, 1960). It is extremely difficult to evaluate the 3D TDGF in an infinite range convolution integral with an oscillate kernel. Basically, there are two main numerical schemes that can be employed for the analysis namely the series expansion in combination with asymptotic expansion and the fourth-order Ordinary Differential Equation (ODE). In accordance with the properties of 3D TDGF in computational domain, Liapis (1986) adopted the series expansion, asymptotic expansion and Filon quadrature in the corresponding regions. King (1987) further extended the use of Bessel function expansion in an additional region. The series expansion, asymptotic expansion and polynomial approximation were employed to solve 3D TDGF (Newman, 1992). The above-mentioned methods actually require numerical experience to determine the partition domain between various computational regions. An improper computational domain subdivision could otherwise lead to a large numerical error in the partition domain.

Additionally, a two-parameter interpolation scheme had been adopted to enhance the efficiency of 3D TDGF for solving the ship

* Corresponding author.
E-mail address: bozhou@dlut.edu.cn (B. Zhou).
Peer review under responsibility of The Society of Naval Architects of Korea.

https://doi.org/10.1016/j.ijnaoe.2020.11.007

hydrodynamics, such as the research work conducted by Huang (1992). On the other hand, Shan et al. (2019) calculated the 3D TDGF and its derivatives using the ascending series expansion and asymptotic expansion, and then presented the residual functions to interpolate the value from that in the precomputed table. The 3D TDGF which was a solution to fourth-order ODE was determined by Clement (1998). Subsequently, Duan and Dai (2001) presented the derivatives of ODE directly for solving the 3D TDGF using the Laplace transform. Based on the mathematical properties of Bessel function, Shen et al. (2007) showed that the 3D TDGF could be represented by the ODE and solved by the fourth-order Runge-Kutta method. However, the fourth-order Runge-Kutta method could lead to a numerical divergence even at a small constant time-step in the numerical computation after long time simulation due to algorithm damping (Tong, 2013).

The solving of ODE using the Taylor series expansion to enhance its accuracy and numerical stability by Chuang et al. (2007) demonstrated that the terms in the equation increased with the time parameter, and were continued to increase as the field and source points closed to the free surface. The solving of the ODE based on the Precise Integration Method (PIM) by Li et al. (2015) was based on the proposal by Zhong (2004), in which the PIM method was shown to provide a better and stable solution than any other numerical methods. However, the comparison of various numerical methods for solving the ODE by Bingham (2016) concluded that the PIM was less efficient and much time-consuming.

In this paper, in order to evaluate the 3D TDGF in a more accurate and efficient manner in the time domain, the computational domain is subdivided into three regions namely the ascending series expansion at small time parameter, the asymptotic expansion at large time parameter, and the Taylor series expansion at moderate time parameter. The properties and the factors affecting the accuracy evaluation of the 3D TDGF are analyzed in detail. The present method for evaluation of 3D TDGF with better accuracy and efficiency is verified compared with the other method (Shan, 2019), especially at moderate time parameter. To further validate the proposed method, the radiation problem for a hemisphere at zero speed is solved by using 3D TDGF method. The computed hydrodynamic coefficients by the proposed method are in good agreement with analytical solutions of Hulme (1982).

2. Numerical expansion of 3D TDGF

2.1. Description of 3D TDGF

A Cartesian coordinate system *oxyz* for the study of 3D TDGF is shown in Fig. 1. In Fig. 1, the *oxy* plane is coincident with mean free surface $z = 0$, and positive z-axis is pointing upwards, and the points $P(x, y, z)$ and $Q(\xi, \eta, \zeta)$ denote as the field and source point respectively. The point$Q'(\xi, \eta, -\zeta)$ is the image of the source point $Q(\xi, \eta, \zeta)$ about the mean free-surface $z = 0$. The parameters$r = |P - Q|$,$r' = |P - Q'|$ and R are the horizontal distances between the field point P and the source point$Q$. The angle θ is between 0 and $\pi/2$, expressing in terms of radian. $G(P, Q; t-\tau)$ of the 3D TDGF in the infinite depth was derived by Wehausen and Laitone (1960) as follows.

$$G(P, Q; t-\tau) = \overline{G}(P, Q)\delta(t-\tau) + \tilde{G}(P, Q;\ t-\tau)H(t-\tau), \tag{1}$$

where $\delta(t)$ is Dirac delta function, $H(t)$ Unit step function, t is instantaneous time, and τ is instantaneous time in time history.

The Rankine $\overline{G}(P, Q)$ and memory $\tilde{G}(P, Q;\ t-\tau)$ parts of TDGF $G(P, Q; t-\tau)$ are

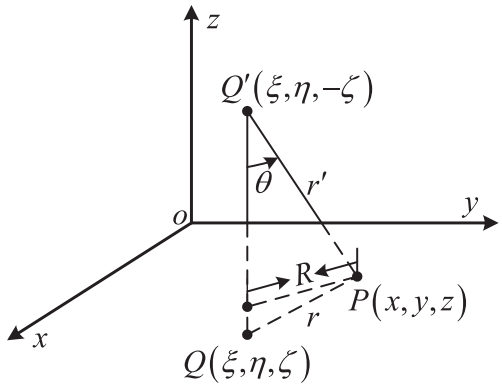

Fig. 1. A Cartesian coordinate system of 3D TDGF.

$$\begin{cases} \overline{G}(P, Q) = 1/r - 1/r' \\ \tilde{G}(P, Q;\ t-\tau) = 2\int_0^\infty \sqrt{gK}\sin\left[\sqrt{gK}\,(t-\tau)\right] e^{K(z+\zeta)} J_0(KR)\,dK \end{cases} \tag{2}$$

where J_0 is Bessel function of zeroth order, K is wave number, and g is gravitational acceleration.

The Rankine part $\overline{G}$ can be integrated over the wet body surface by using the Hess-Smith method (Hess and Smith, 1964). Considering $\lambda = Kr'$, $\mu = -(z+\zeta)/r'$ and $\beta = \sqrt{g/r'}(t-\tau)$, the memory part of TDGF in Eq. (2) can be written in terms of μ and β as follows.

$$\begin{cases} \tilde{G}(P, Q;\ t-\tau) = 2\sqrt{g/r'^3}F(\mu, \beta) \\ F(\mu, \beta) = \int_0^\infty \sqrt{\lambda}\sin\left(\beta\sqrt{\lambda}\right) e^{-\lambda\mu} J_0\left(\lambda\sqrt{1-\mu^2}\right) d\lambda \end{cases} \tag{3}$$

The main objective in the computational domain $(0 \le \beta \le \infty 0 \le \mu \le 1)$ is to compute the function. With reference to the research study of Clement (1998), $F(\mu, \beta)$ is the solution of the following fourth-order Ordinary Differential Equation (ODE).

$$\frac{\partial^4 F(\mu,\beta)}{\partial\beta^4} + \mu\beta\frac{\partial^3 F(\mu,\beta)}{\partial\beta^3} + \left(\frac{1}{4}\beta^2 + 4\mu\right)\frac{\partial^2 F(\mu,\beta)}{\partial\beta^2} + \frac{7}{4}\beta\frac{\partial F(\mu,\beta)}{\partial\beta} + \frac{9}{4}F(\mu,\beta) = 0. \tag{4}$$

The initial conditions for Eq. (4) are derived as follows.

$$\begin{cases} \dfrac{\partial^{(2k)} F(\mu,0)}{\partial\beta^{(2k)}} = 0 \\ \dfrac{\partial^{(2k+1)} F(\mu,0)}{\partial\beta^{(2k+1)}} = (-1)^k (k+1) P_{k+1}(\mu) \end{cases}, k = 0, 1, \cdots, \tag{5}$$

where$P_{k+1}(\bullet)$ is the Legendre polynomial of order k+1.

2.2. Taylor series expansion

A set of four first-order ODE are derived to solve Eq. (4) from the vector $\tilde{\mathbf{x}} = \left[F, \frac{\partial F(\mu,\beta)}{\partial\beta}, \frac{\partial^2 F(\mu,\beta)}{\partial\beta^2}, \frac{\partial^3 F(\mu,\beta)}{\partial\beta^3}\right]^T$ as shown below.

$$\dot{\tilde{\boldsymbol{x}}}(\beta)=\tilde{\boldsymbol{A}}(\beta)\tilde{\boldsymbol{x}}(\beta),\tilde{\boldsymbol{A}}(\beta)=\begin{bmatrix}0 & 1 & 0 & 0\\ 0 & 0 & 1 & 0\\ 0 & 0 & 0 & 1\\ -\frac{9}{4} & -\frac{7}{4}\beta & -\left(4\mu+\frac{\beta^2}{4}\right) & -\mu\beta\end{bmatrix}. \tag{6}$$

For the time marching of Eq. (6), the initial condition is a fixed value of μ from Eq. (5). $\Delta\beta=\beta_{k+1}-\beta_k$ is denoted as a time step ($k=0,1,2,\cdots$). The solution to Eq. (4) is based on the Taylor series expansion of $F(\mu,\beta)$ with starting time β_k proposed as

$$F(\beta)=\sum_{n=0}^{N}a_n(\beta-\beta_k)^n, \tag{7}$$

where N is the order of polynomial expansion.

Eq. (7) is added to ODE, and the terms in the equation are determined at each power of β. The coefficient a_n can be solved based on the initial values of vector $\tilde{\mathbf{x}}(\beta_k)$ using the recursive algorithm (Chuang et al., 2007). The $F(\beta)$ can be obtained by adding a_n into Eq. (7).

2.3. Series expansion for small values of β

The auxiliary function $f(p)$ can be expressed as follows.

$$f(p)=\int_0^\infty \lambda^p \mathrm{e}^{\mathrm{i}\beta\lambda^{1/2}}\mathrm{e}^{-\lambda\cos\theta}J_0(\lambda\sin\theta)\mathrm{d}\lambda. \tag{8}$$

At $p=\frac{1}{2}$, the relationship of the functions $F(\mu,\beta)$ and $f(p)$ is. $F(\mu,\beta)=\mathrm{Im}[f(1/2)]$

For a lower value of β and at zero as an assumption, the factor $\mathrm{e}^{\mathrm{i}\beta\lambda^{1/2}}$ of $f(1/2)$ can be expanded as an ascending power series that each term can be solved by integration. Thus, $f(1/2)$ can be expressed by Huang (1992) as follows.

$$f(1/2)=\sum_{n=0}^{\infty}\frac{(\mathrm{i}\beta)}{n!}\Gamma\left(\frac{n}{2}+\frac{3}{2}\right)P_{\frac{n}{2}+\frac{1}{2}}(\cos\theta), \tag{9}$$

where $\Gamma(\cdot)$ is Gamma function.

Substituting Eq. (10) into Eq. (9), the series expansion of $F(\mu,\beta)$ can be derived as,

$$F(\mu,\beta)=\sum_{n=0}^{\infty}(-1)^n\beta^{2n+1}\frac{(n+1)!}{(2n+1)!}P_{n+1}(\mu) \tag{10}$$

2.4. Asymptotic expansion for large values of β

For a large value of β, the asymptotic expansions are adopted to evaluate the 3D TDGF. The integral part of $f(p)$ can be re-arranged by substituting $\lambda=\varpi^2$, as proposed by Sun (2009), and then decomposes to a form of,

$$\begin{aligned}f(p)&=2\int_0^\infty \varpi^{2p+1}\mathrm{e}^{\mathrm{i}\beta\varpi}\mathrm{e}^{-\varpi^2\cos\theta}J_0\left(\varpi^2\sin\theta\right)\mathrm{d}\varpi\\&=f_0(p)+f_1(p)+f_2(p),\end{aligned} \tag{11}$$

where

$$\begin{cases}f_0(p)=2\int_0^{\frac{\mathrm{i}\beta}{2}}\varpi^{2p+1}\mathrm{e}^{\mathrm{i}\beta\varpi}\mathrm{e}^{-\varpi^2\cos\theta}J_0\left(\varpi^2\sin\theta\right)\mathrm{d}\varpi\\ f_{1,2}(p)=2\int_{\frac{\mathrm{i}\beta}{2}}^{\infty}\varpi^{2p+1}\mathrm{e}^{\mathrm{i}\beta\varpi}\mathrm{e}^{-\varpi^2\cos\theta}H_0^{(1,2)}\left(\varpi^2\sin\theta\right)\mathrm{d}\varpi\end{cases}, \tag{12}$$

where $H_0^{(1,2)}(\cdot)$ is the Hankel function $J_0(\cdot)\pm\mathrm{i}Y_0(\cdot)$, and $H_0^{(1,2)}(\varpi^2\sin\theta)$ can be obtained from the following formulation.

$$H_0^{(1,2)}\left(\varpi^2\sin\theta\right)=\mathrm{e}^{\pm\mathrm{i}(\varpi^2\sin\theta-\pi/4)}\sqrt{\frac{2}{\pi\varpi^2\sin\theta}}\sum_{n=0}^{\infty}c_n\left(\frac{\pm\mathrm{i}}{\varpi^2\sin\theta}\right)^n, \tag{13}$$

where $c_n=[\Gamma(n+1/2)]^2/\pi 2^n n!$.

The integral of $f_0(p)$ can be expanded by using the Watson's Lemma method as shown below.

$$f_0(p)\simeq 2\mathrm{i}^{2p+2}\sum_{n=0}^{\infty}\frac{(2n+2p+1)}{\beta^{2n+2p+2}n!}P_n(\cos\theta). \tag{14}$$

The $f_{1,2}(p)$ can be solved by using the stationary phase method (Newman, 1992) in which $f_1(p)$ is ignored. The final expression of function $f_2(p)$ can thus be expressed as follows.

$$f_2(p)\simeq 2(2\sin\theta)^{-1/2}\mathrm{e}^{-\beta^2\cos\theta/4}\sum_{n=0}^{\infty}\frac{1}{\sin^n\theta}\sum_{m=0}^{\infty}d_{nm}\mathrm{e}^{\mathrm{i}\theta_{nm}}\left(\frac{2}{\beta}\right)^{2m+2n-2p}, \tag{15}$$

where $d_{nm}=\frac{c_n(2p-2n)!}{(2p-2m-2n)!2^{2m}m!}, 2p-2n>0$; $d_{nm}=\frac{c_n(2m+2n-2p-1)!}{(2n-2p-1)!2^{2m}m!}, 2p-2n\le 0$; and $\theta_{nm}=\frac{\beta^2}{4}\sin\theta+\left(p-m-\frac{n}{2}+\frac{1}{4}\right)\pi+\left(m+2n-2p-\frac{1}{2}\right)\theta$.

2.5. Comparison of various expansion methods

A comparison of the three methods to evaluate the 3D TDGF, namely the series, the asymptotic and the Taylor serious expansion methods is conducted and summarized in Table 1.

3. Numerical results and discussion

3.1. Accuracy evaluation of 3D TDGF

To validate the numerical results generated by the proposed method (referred as "Present method"), the analytical expressions of $F(0,\beta)$ and $F(1,\beta)$ were referenced to the research work of Clement (1998). The analytical expressions of $F(0,\beta)$ and $F(1,\beta)$ are as follows.

Table 1
Comparison of three expansion methods.

	Series expansions	Asymptotic expansions	Taylor series expansions
Scope of application	Small values of β	Large values of β	All computational domain
Factors affecting accuracy	μ ,β and truncated number n_0 of Eq. (10)	μ ,β,truncated number n_0 of Eq. (14) and truncated number n_0)of Eq. (15)	(m_0, μ,β,the order of polynomial expansion N and time step $\Delta\beta$

$$F(0,\beta)=\frac{\pi\beta^3}{16\sqrt{2}}\left[J_{1/4}\left(\beta^2/8\right)J_{-1/4}\left(\beta^2/8\right)+J_{3/4}\left(\beta^2/8\right)J_{-3/4}\left(\beta^2/8\right)\right], \tag{16}$$

and

$$F(1,\beta)=\beta e^{-\beta^2/4}M\left(-1/2,3/4,\beta^2/4\right), \tag{17}$$

where J_ν and M are Bessel function of order ν and Confluent hypergeometric function respectively.

The study cases of the numerical analysis at $\mu = 0$,$\mu = 0.5$ and $\mu = 1$ are considered. The exact results of 3D TDGF computed by the analytical formulas are denoted as "Analytical method" (Clement, 1998). Since there is no analytical expression of 3D TDGF for the case $\mu = 0.5$, the numerical results of 3D TDGF is obtained by the PIM method (Li et al., 2015). The main feature of the PIM method is that a high degree of accuracy can be achieved without considering the efficiency. In the current numerical analysis, the parameters of the PIM method are set at $m = 50$ and $N = 20$ with constant time step $\Delta\beta = 0.05$. The order of magnitude of absolute errors of $F(\mu,\beta)$ between the "Analytical method" and the PIM method is $O(10^{-10})$.

For the method using the series expansion at time parameter $0 \le \beta \le 10$ as shown in Figs. 2–4, the accuracy of the 3D TDGF decreases with increasing β. The truncated number n_0 increases at large β value of 10 and higher. At large β, a tendency on the occurrence of divergence in numerical results is specifically noted. Similarly, for the method of using the asymptotic expansion at $\beta \ge 10$ as shown in Figs. 5–7, the accuracy of the 3D TDGF also increases with increasing β. But the convergence of numerical results occurs at truncated numbers $m_0 \ge 3$ and $n_0 \ge 3$.

There is a need to note that the function $f_1(p)$ is ignored in the evaluation of the 3D TDGF using the asymptotic expansion. As β approaches 10, the error becomes significant and the function $f_1(p)$ forms a smaller part of 3D TDGF that could improve its accuracy. Since only the asymptotic expansion $f_0(p)$ can be used to compute the 3D TDGF, the error in the numerical analysis at $\mu = 1$ is therefore significant.

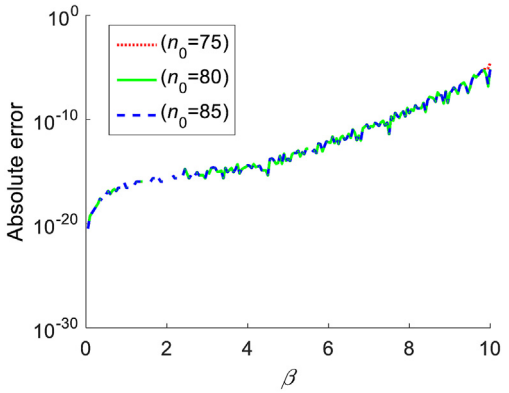

Fig. 2. Absolute errors of $F(0,\beta)$ between "Analytical method" and series expansion.

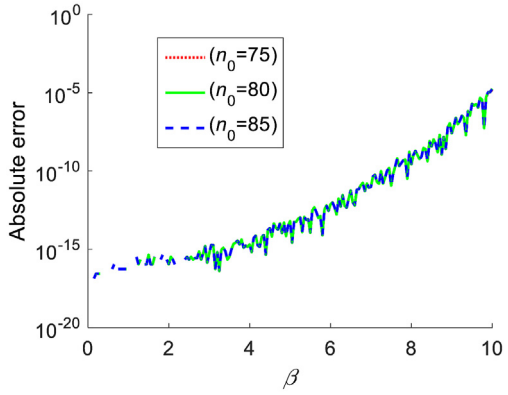

Fig. 3. Absolute errors of $F(0.5,\beta)$ between PIM method and series expansion.

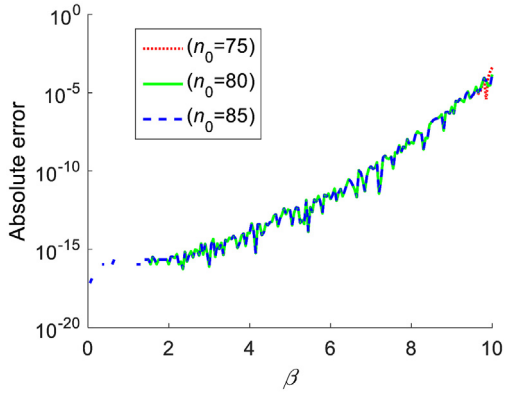

Fig. 4. Absolute errors of $F(1,\beta)$ between "Analytical method" and series expansion.

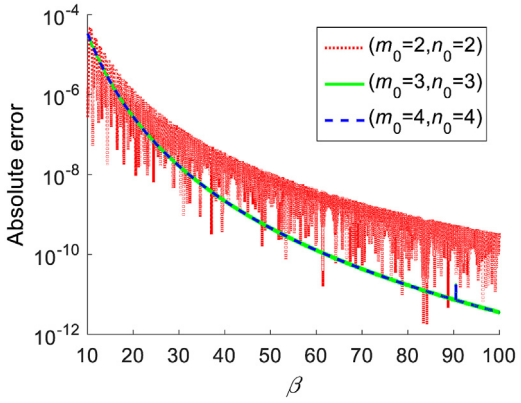

Fig. 5. Absolute errors of $F(0,\beta)$ between "Analytical method" and asymptotic expansion.

The absolute errors generated among the three methods at time step $\Delta\beta = 0.05$, namely the analytical method, the PIM method and

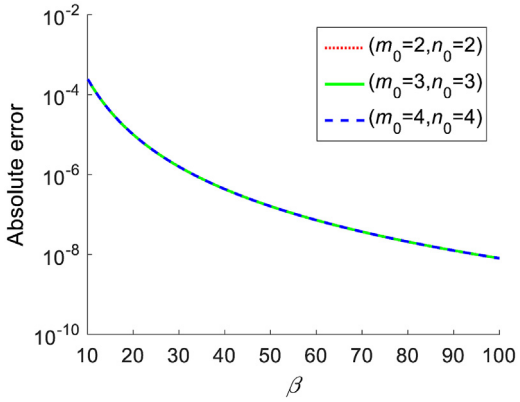

Fig. 6. Absolute errors of $F(0.5,\beta)$ between PIM method and asymptotic expansion.

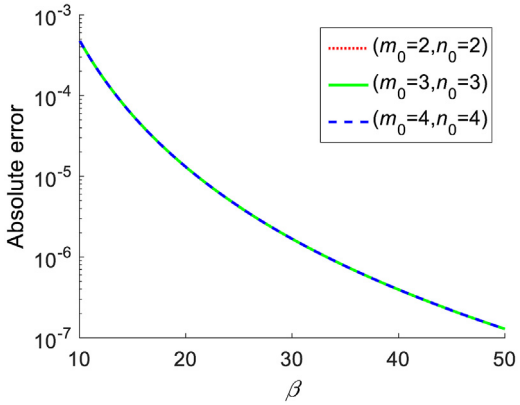

Fig. 7. Absolute errors of $F(1,\beta)$ between "Analytical method" and asymptotic expansion.

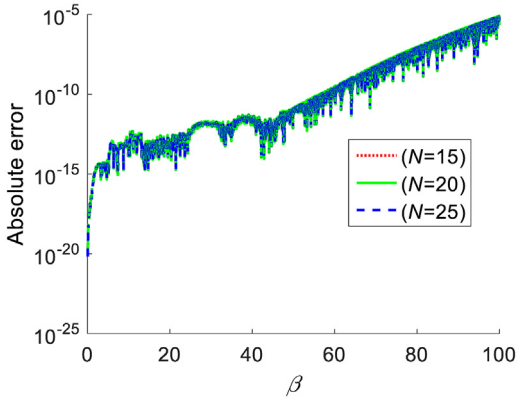

Fig. 8. Absolute errors of $F(0,\beta)$ between "Analytical method" and Taylor series expansion.

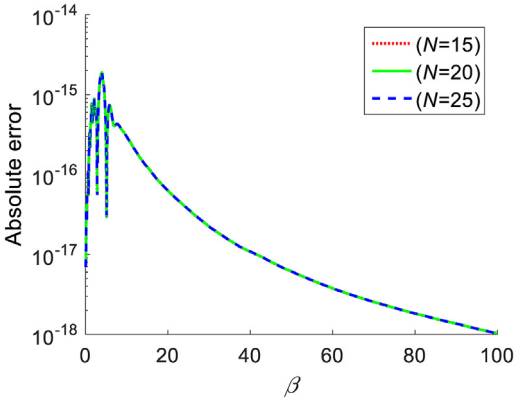

Fig. 9. Absolute errors of $F(0.5,\beta)$ between PIM method and Taylor series expansion.

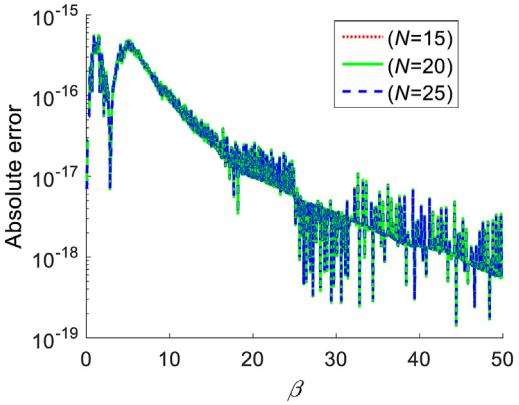

Fig. 10. Absolute errors of $F(1,\beta)$ between "Analytical method" and Taylor series expansion.

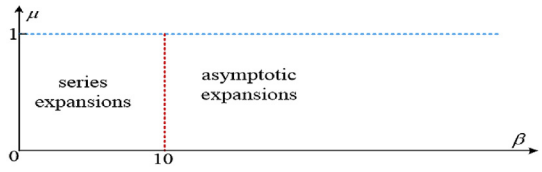

Fig. 11. Algorithm for evaluation of $F(\mu,\beta)$ proposed by Shan et al. (2019).

the Taylor series expansion are plotted in Figs. 8–10. At $\mu = 0$, the amplitude and oscillating frequency of the 3D TDGF increases rapidly with β, but the evaluation accuracy decreases. At $\mu = 1$, the amplitude and oscillating frequency of the 3D TDGF decreases rapidly but with increasing β and increasing in accuracy. At a constant time step, the accuracy evaluation of the 3D TDGF increases with the order of polynomial expansion N.

For the method proposed by Shan et al. (2019) (referred as "Shan's method") at $0 \le \beta \le 10$ as shown in Fig. 11, the truncated number n of Eq. (10) by using the method of series expansion is 85. On the other hand for the case of $\beta > 10$, the truncated number n_0 of $f_0(p)$ by using the method of asymptotic expansion is 5, and the truncated number (m_0, n_0) of $f_2(p)$ is (4, 4).

For the case of $0 \le \beta \le 10$ as shown in Fig. 12, the accuracy of $F(\mu,\beta)$ decreases with increasing β and the order of accuracy can be as low as 10^{-5}. At higher value of $10 < \beta < 40$, the order of accuracy reduces to $O(10^{-4})$ as μ gradually reach a constant 1.0. The reason is that the function $f_1(p)$ is omitted in the evaluation of $F(\mu,\beta)$. At even higher value of $40 < \beta$, the influence on the omission of $f_1(p)$ in the evaluation of $F(\mu,\beta)$ is neglected, and thus the absolute errors of $F(\mu,\beta)$ between the PIM method and the Shan's method is $O(10^{-7})$.

In order to improve the accuracy of the 3D TDGF based on the Shan's method and the "Present method" as shown in Fig. 13, the polynomial order N of 20 in Eq. (7) for $8 \le \beta \le 50$, the series expansion for $0 \le \beta \le 8$ and the asymptotic expansion for $\beta > 50$ are considered.

For the method of using the Taylor series expansion with the

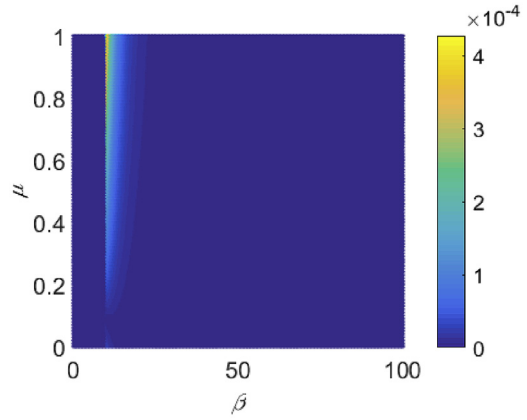

Fig. 12. Absolute errors of $F(\mu,\beta)$ between PIM method and Shan's method.

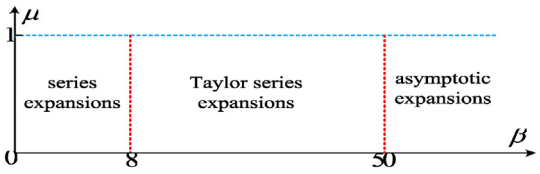

Fig. 13. Current proposed algorithm for evaluation of.$F(\mu,\beta)$

order of polynomial $N = 20$ at$8 \le \beta \le 50$, as presented in Fig. 14, the absolute errors of $F(\mu,\beta)$ between the PIM method and

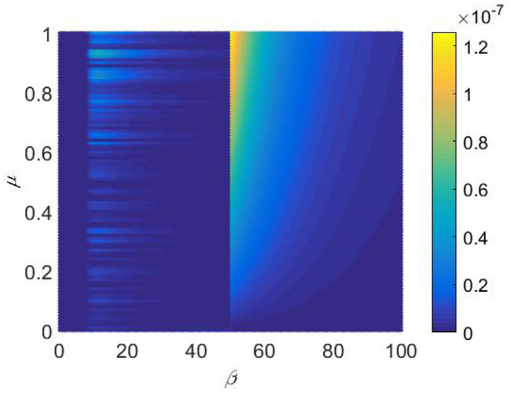

Fig. 14. Absolute errors of $F(\mu,\beta)$ between PIM method and "Present method".

the"Present method" can be $O(10^{-8})$. The accuracy of the 3D TDGF improved by a magnitude order of 2 in comparison to that of the "Shan's method". In the computational domain, the absolute errors of $F(\mu,\beta)$ between the PIM method and the"Present method" can also be $O(10^{-7})$.

From these figures, the time the PIM method, the "Present method" and the "Shan's method" generate the 3D TDGF for$0 \le \mu \le 1$ and $0 \le \beta \le 250$ at 201×5001 sets of (μ,β) is 23,927.4s, 1279.4s and 1547.2s, respectively. The computation is run on the computer platform of Intel(R) Core (TM) i5-9400F and CPU 2.90 GHz. The comparison of the results revealed that the accuracy evaluation of the 3D TDGF by the "Present method" is the most efficient.

3.2. The hemisphere case study

Further, a case study to examine the accuracy of the "Present method" based on a floating hemisphere is conducted. A constant panel method is commonly used to solve the radiation wave problem of floating structures, such as the floating hemisphere currently considered in the study, at zero speed. The boundary value equations and governing equations for perturbation velocity potential are given in the reference (Li et al., 2015). The added mass and damping coefficient can be obtained after solving the perturbation velocity potential (Beck and Liapis, 1987). For the study, the non-dimensional form of heave added mass A_{33} and damping coefficient B_{33} are given as $A'_{33} = \frac{A_{33}}{\rho\nabla}$ and $B'_{33} = \frac{B_{33}}{\omega\rho\nabla}$ respectively, where ∇ the hemisphere displacement volume,ρ is density of fluid, and ω the wave circular frequency. The wave number is represented as KR. In the simulation, the floating hemisphere is modelled with 456 panels for analysis. As plotted in Fig. 15, the relative errors of the heave added mass and damping coefficients between the "Present method" and the analytical solutions proposed by Hulme (1982) are within 3%.

4. Conclusion

In this paper, the accuracy evaluation of the 3D TDGF is carried out in the computational domain that consists of three subdomains namely the ascending series expansion, the Taylor series expansion and the asymptotic expansion. A new subdivision method is proposed based on the properties of 3D TDGF in the computational domain in which the time parameter can be taken as $8 \le \beta \le 50$. The results showed that the "Present method" improves the accuracy of the 3D TDGF in an order of magnitude of two in comparison to that of the Shan's method (Shan et al., 2019). The "Present method" also demonstrates a 17.3% higher efficiency, with

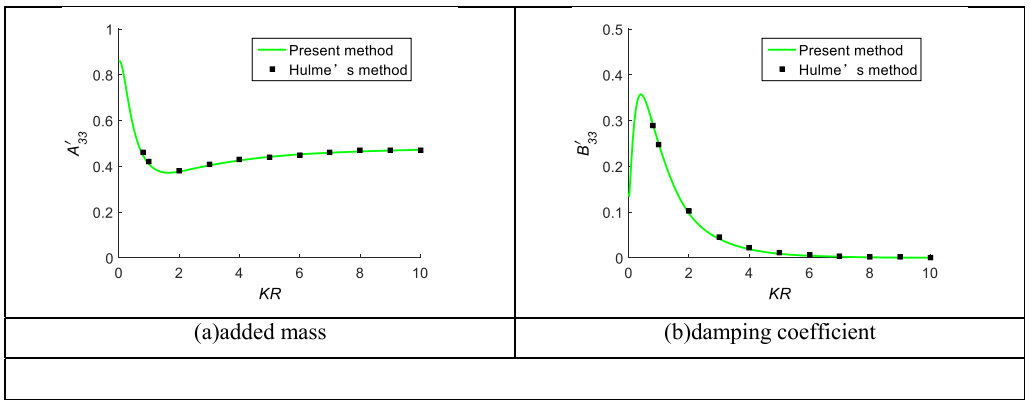

Fig. 15. Heave hydrodynamic coefficients of the hemisphere.

parameters in the range of $0 \leq \mu \leq 1$ and $0 \leq \beta \leq 250$ at 201×5001 sets of (μ,β), than the Shan's method. The hydrodynamic analysis of the floating hemisphere at zero speed based on the TDGF method showed that the "Present method" is in good agreement with that of the analytical solution of Hulme (1982) with a difference of less than 3%.

Declaration of competing interest

The authors declare that they have no known competing financial interests or personal relationships that could have appeared to influence the work reported in this paper.

Acknowledgement

This research is supported by the LiaoNing Revitalization Talents Program (No. XLYC1807190, XLYC1908027); National Natural Science Foundation of China (No. 52071059).

References

Beck, R., Liapis, S., 1987. Transient motions of floating bodies at zero forward speed. J. Ship Res. 31 (3), 164–176.
Bingham, H.B., 2016. A note on the relative efficiency of methods for computing the transient free-surface Green function[J]. Ocean. Eng. 120, 15–20.
Chuang, J.M., Qiu, W., Peng, H., 2007. On the evaluation of the time-domain Green function. Ocean. Eng. 34, 962–969.
Clement, A.H., 1998. An ordinary differential equation for green function of time-domain free-surface hydrodynamics. J. Eng. Math. 33 (2), 201–217, 1998.
Datta, R., Rodrigues, J.M., Soares, C.G., 2011. Study of the motions of fishing vessels by a time domain panel method. Ocean. Eng. 38 (5), 782–792.
Duan, W.Y., Dai, Y.S., 2001. New derivation of ordinary differential equations for transient free-surface Green functions. China Ocean Eng. 4, 499–507.
Hess, J.L., Smith, A.M.O., 1964. Calculation of non-lifting potential flow about arbitrary three-dimensional bodies. J. Ship Res. 8 (2), 22–44.
Huang, D.B., 1992. Approximation of time-domain free surface function and its spatial derivatives. Shipbuilding of China 2, 16–25.
Hulme, A., 1982. The wave forces acting on a floating hemisphere undergoing forced periodic oscillations. J. Fluid Mech. 121, 443–463.
King, B.W., 1987. Time Domain Analysis of Wave Exciting Forces on Ships and Bodies. Ph.D. Thesis. The University of Michigan, Ann Arbor, Michigan.
Liapis, S.J., 1986. Time Domain Analysis of Ship Motions. Ph.D. Thesis. The University of Michigan, Ann Arbor.
Li, Z.F., Ren, H.L., Tong, X.W., Li, H., 2015. A precise computation method of transient free surface Green function. Ocean. Eng. 105, 318–326.
Newman, J.N., 1992. The approximation of free-surface Green functions. In: Martin, P.A., Wickham, G.R. (Eds.), Wave Asymptotics. Cambridge University Press, Cambridge, UK, pp. 107–135.
Shan, P.H., Wang, Y.H., Wang, F.H., Wu, J.M., Zhu, R.C., 2019. An efficient algorithm with new residual functions for the transient free surface green function in infinite depth. Ocean. Eng. 178, 435–441.
Shen, L., Zhu, R.C., Miao, G.P., Liu, Y.Z., 2007. A practical numerical method for deep water time domain in Green function. Chinese Journal of Hydrodynamics 3, 380–386.
Singh, S.P., Sen, D., 2007. A comparative linear and nonlinear ship motion study using 3-D time domain methods. Ocean. Eng. 34 (13), 1863–1881.
Sun, L., 2009. A Study of Ship-Generated Waves and its Effects on Structures. Ph.D.Thesis. The Dalian University of Technology, Dalian.
Sun, W., Ren, H.L., 2018. Ship motions with forward speed by time-domain Green function method. Chinese Journal of Hydrodynamics 33 (2), 216–222.
Tong, X.L., 2013. Three Dimensional Time Domain Hybrid Method for Ship and Marine Structure Motions. Ph.D.Thesis. Harbin Engineering University, Harbin.
Wehausen, J.V., Laitone, E.V., 1960. Surface Waves. Encyclopedia of Physics, Vol. IX/Fluid Dynamics III. Springer-Verlag, Berlin, pp. 446–778.
Zhang, G.Y., Wang, S.Q., Sui, Z.X., Sun, L., Zhang, Z.Q., Zong, Z., 2019. Coupling of SPH with smoothed point interpolation method for violent fluid structure interaction problems. Eng. Anal. Bound. Elem. 103, 1–10.
Zhong, W.X., 2004. On precise integration method. J. Comput. Appl. Math. 163, 59–78.